Stimulated-Raman-adiabatic-passage–like transitions in a harmonically modulated optical lattice

Benjamin P. Holder and Linda E. Reichl
Center for Complex Quantum Systems and Department of Physics, The University of Texas at Austin, Austin, Texas 78712, USA
(Received 26 February 2007; published 26 July 2007)

We introduce a method for the coherent acceleration of atoms trapped in an optical lattice, using the well-known model for stimulated Raman adiabatic passage (STIRAP). Specifically, we show that small harmonic modulations of the optical lattice amplitude, with frequencies tuned to the eigenvalue spacings of three "unperturbed" eigenstates, reveals a three-state STIRAP subsystem. We use this model to realize an experimentally achievable method for transferring trapped atoms from stationary to motional eigenstates.

DOI: 10.1103/PhysRevA.76.013420 PACS number(s): 42.50.Vk, 03.75.Be, 05.45.Mt

I. INTRODUCTION

Stimulated Raman adiabatic passage (STIRAP) is a method for achieving coherent transitions between quantum states by applying two coupling fields in a nonintuitive pulse sequence. The frequencies of these fields are tuned to the eigenvalue spacings between the "initial" and "target" states and a third "intermediate" state. When the coupling of the target and intermediate states precedes that of the initial and intermediate states in time, population transfer from the initial to target state is achieved. In the adiabatic limit, the transition is 100% efficient and involves no occupation of the intermediate state. The use of STIRAP for atomic and molecular systems was first demonstrated experimentally by Gaubatz and co-workers [1,2], who achieved population transfer between vibrational levels in a beam of sodium molecules. Further references on the STIRAP transitions in atoms and molecules can be found in the review by Vitanov *et al.* [3]. In atom optics experiments, STIRAP has been used for coherent momentum transfer [4–6], and velocity-selective coherent population trapping for laser cooling of trapped atoms [7,8]. Extensions of STIRAP, with a particular focus on the influence of quantum chaos, have been studied by Na and Reichl [9,10]. Na *et al.* [11] have also used STIRAP to control the isomerization transition of HOCl.

As a theoretical model, STIRAP can be defined by the adiabatic behavior of a three-level system, which in some basis $(|a\rangle,|b\rangle,|c\rangle)$ is represented by the Hamiltonian

$$H(t') = -\frac{\hbar}{2}\begin{pmatrix} 0 & W_1(t') & 0 \\ W_1(t') & -2\Delta & W_2(t') \\ 0 & W_2(t') & 0 \end{pmatrix}, \tag{1}$$

under the variation of W_1 and W_2 via the dimensionless parameter t', with Δ a constant. This model, which we refer to as the "STIRAP model" hereafter, was first introduced by Kuklinski *et al.* [12], following significant work by Hioe *et al.* [13–15], to succinctly describe the experimental results of Gaubatz *et al.* [1]. Starting from a system in which the pairs of states $(|a\rangle,|b\rangle)$ and $(|b\rangle,|c\rangle)$ are each dipole-coupled by monochromatic electric fields, the STIRAP model is derived by applying the rotating-wave approximation and assuming an equal detuning of the coupling frequencies Δ (see Fig. 1). In that particular system the W_i are the Rabi oscillation frequencies corresponding to the two couplings. The STIRAP transition, however, does not depend on the physical system from which Eq. (1) is derived. In an application of this model by Eckert *et al.* [16], for example, the functions $W_i(t')$ were related to the spatial separations of three optical microtraps in order to induce coherent transport of atoms between the ground states of the two farthest separated traps.

The matrix in Eq. (1) allows for a transition of the type described above because of the existence of the eigenvector

$$|1(t')\rangle = \cos\theta(t')|a\rangle - \sin\theta(t')|c\rangle, \tag{2}$$

where $\tan\theta(t') \equiv \frac{W_1(t')}{W_2(t')}$. Under the conditions

$$\lim_{t'\to-\infty}\frac{W_1(t')}{W_2(t')} \to 0 \quad \text{and} \quad \lim_{t'\to+\infty}\frac{W_2(t')}{W_1(t')} \to 0, \tag{3}$$

the adiabatic evolution of state $|1\rangle$ is from $|a\rangle$ to $|c\rangle$. Thus, the transition is achieved by first coupling the upper two levels and then coupling the lower two (in some continuous, e.g., Gaussian, manner). Moreover, because of the form of the eigenvector $|1\rangle$, the state $|b\rangle$ remains unoccupied throughout the transition.

In this paper, we apply the method of STIRAP to the motional states of atoms in an optical lattice. As was shown by Graham, Schlautmann, and Zoller [17], the interaction of a single transition in an alkali atom with a pair of counterpropagating lasers can be reduced to an effective Hamiltonian for the center-of-mass motion of the atom in a cosine potential. Modulation of the laser amplitudes and/or the introduction of laser pairs with offset frequencies introduces a periodic time dependence (see Appendix A). Here we will analyze the "two-resonance" system described by the effective Hamiltonian

$$\hat{H}_0(t) = \hat{p}^2 + \kappa_0[\cos\hat{x} + \cos(\hat{x} - \omega_0 t)], \tag{4}$$

where each of the two cosine terms are produced by a pair of counterpropagating lasers with κ_0 proportional to the square of the laser amplitudes (here and throughout this paper we use the dimensionless variables defined in Appendix A). We show, using perturbation analysis of an associated Floquet Hamiltonian, that small harmonic modulations of the laser amplitudes can be used to affect a STIRAP-like transition of a state localized in the stationary cosine well into a state localized in the traveling cosine well. Thus, atoms trapped in a stationary optical lattice are coherently transferred into a

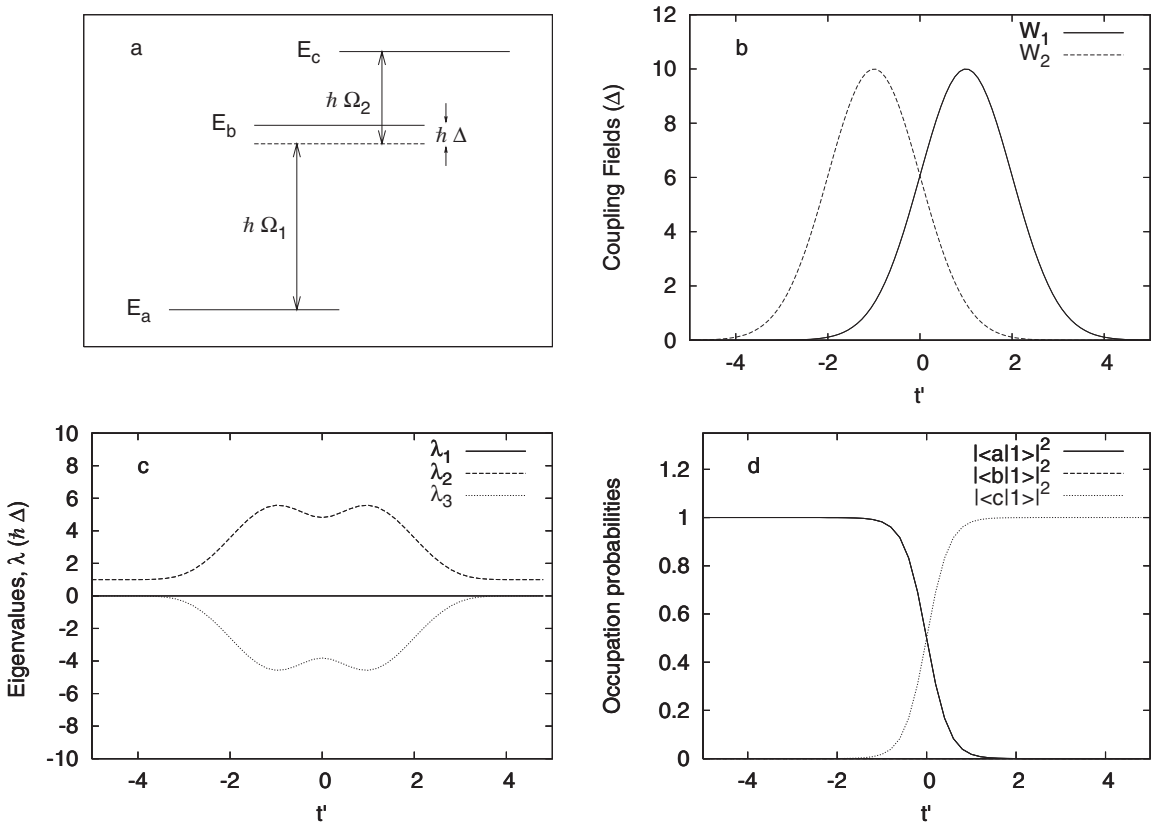

FIG. 1. The three-level "ladder" STIRAP system [Eq. (1)] with maximum coupling strength $\max[W_1(t')]=\max[W_2(t')]=10\Delta$. Coupling fields are applied with frequencies equally detuned from the spacings of the unperturbed energy levels by Δ (a). Adiabatic variation of the amplitudes of the coupling fields over the dimensionless parameter t' (b) in the manner described by Eq. (3) affects a transition of the $|1\rangle$ eigenvector between basis states $|a\rangle$ and $|c\rangle$ (d). The eigenvalue corresponding to this state remains unchanged at zero throughout the transition (c).

traveling lattice with dimensionless velocity ω_0.

In Sec. II we present an analysis of the time-independent "quantum pendulum" system which reveals a three-level STIRAP model in the regime of small perturbation. Section III contains a slightly modified method in order to obtain a STIRAP-like model for the time-dependent "two-resonance" system. In each case, adiabatic results are compared to numerical evolution of the Schrödinger equation and transitions of nearly 100% efficiency are observed. Concluding remarks are presented in Sec. IV.

II. STIRAP TRANSITIONS IN THE QUANTUM PENDULUM

Before analyzing the two-resonance effective Hamiltonian presented in the introduction, we will consider STIRAP-like transitions within the quantum pendulum system,

$$\hat{H}_{\text{pend}} = \hat{p}^2 + \kappa_0 \cos \hat{x}. \tag{5}$$

This is the simplest type of effective Hamiltonian for optical lattice experiments, achieved with a single pair of counterpropagating lasers with equal frequencies. The parameter κ_0 is proportional to the square of the electric field amplitude. Because of experimental techniques which can limit the dimensionless momentum values to the integers (see Appendix A), the eigenstates can be considered spatially periodic with period 2π. The position space solutions to the eigenvalue equation $\hat{H}_{\text{pend}}|\chi_n\rangle = E_n|\chi_n\rangle$ are the Mathieu functions $\langle x|\chi_n\rangle$ $(n \in Z)$ [18], with n even labeling even-parity functions and n odd labeling odd-parity functions.

To affect a transition in this system using STIRAP, we add a time-periodic modulation of the lattice amplitude of the form

$$\lambda \hat{V}(t) = \lambda \cos \hat{x}[\kappa_1 \cos(\Omega_1 t) + \kappa_2 \cos(\Omega_2 t)], \tag{6}$$

where λ is small, and Ω_1 and Ω_2 are commensurate with $\frac{\Omega_1}{\Omega_2} = \frac{m_1}{m_2}$ $(m_i \in Z)$. It is useful to write Ω_1 and Ω_2 in terms of a common frequency ω such that $\Omega_1 = m_1\omega$ and $\Omega_2 = m_2\omega$, where $\omega = \frac{2\pi}{T}$ and T is the periodicity of the perturbation. This perturbation is achieved experimentally by modulating the intensity of the counterpropagating laser radiation about the κ_0 value, meaning that the lasers' electric field amplitude $E(t)$ should take the form

$$|E(t)|^2 \sim \kappa_0 + \lambda[\kappa_1 \cos(m_1\omega t) + \kappa_2 \cos(m_2\omega t)]. \tag{7}$$

For now, we will consider the coefficients κ_1 and κ_2 to have constant values. Perturbation analysis will reveal that, for small values of λ, there exists a three-state subsystem identical to the STIRAP model, parametrized by these coeffi-

cients. A STIRAP-type transition can then be affected by adiabatic variation of κ_1 and κ_2 in the manner described in Eq. (3). The justification of this time parametrization of the κ_i, following a Floquet analysis of the system where they are considered constant, is provided in Appendix B.

Having required that the frequencies Ω_1 and Ω_2 are commensurate, we can analyze the dynamics of the full system

$$i\frac{\partial}{\partial t}|\psi(t)\rangle = [\hat{H}_{\text{pend}} + \lambda\hat{V}(t)]|\psi(t)\rangle, \tag{8}$$

using Floquet theory, which we review briefly here. Any solution of Eq. (8) can be written in the form

$$|\psi_\alpha(t)\rangle = e^{-i\epsilon_\alpha t}|\phi_\alpha(t)\rangle, \tag{9}$$

where the *Floquet eigenstate* $|\phi_\alpha(t)\rangle$ is periodic in time with period T, and ϵ_α is called the *Floquet eigenvalue*. Plugging this solution into the Schrödinger equation we arrive at the eigenvalue equation

$$\hat{H}_F|\phi_\alpha\rangle \equiv \left(\hat{H}_{\text{pend}} + \lambda\hat{V}(t) - i\frac{\partial}{\partial t}\right)|\phi_\alpha\rangle = \epsilon_\alpha|\phi_\alpha\rangle, \tag{10}$$

where the *Floquet Hamiltonian* $\hat{H}_F$ is a Hermitian operator in an extended Hilbert space which has time as a periodic *coordinate* [19–21]. Diagonalization of $\hat{H}_F$ in some convenient basis in this space yields the Floquet eigenstates and eigenvalues. The Floquet eigenstates have an infinite multiplicity with respect to the solutions of the Schrödinger equation in the sense that for any Floquet eigenstate $|\phi(t)\rangle$ with eigenvalue ϵ, there exists another solution $|\tilde{\phi}(t)\rangle = e^{iQ\omega t}|\phi(t)\rangle$ $(Q \in \mathbb{Z})$ with eigenvalue $\tilde{\epsilon} = \epsilon + Q\omega$. These two Floquet states are, however, associated to the same physical state, i.e., $|\psi(t)\rangle \equiv e^{-i\epsilon t}|\phi(t)\rangle = e^{-i\tilde{\epsilon}t}|\tilde{\phi}(t)\rangle$. The implication of this fact is that the dynamics of the physical system can be understood by considering only those Floquet states whose eigenvalues appear in a single "zone" $\epsilon^\star \leqslant \epsilon < \epsilon^\star + \omega$, labeled by the constant $\epsilon^\star$.

The STIRAP model system is derived by applying perturbation theory to Eq. (10), where the two frequencies in $\hat{V}(t)$ are chosen to "couple" three pendulum eigenvalues, at a particular value of κ_0, in the manner shown in Fig. 1(a). Although, in general, the ratio of these eigenvalue spacings is not rational, the equal detuning Δ allows for Ω_1 and Ω_2 to be chosen as commensurate. More precisely, given three eigenvalues of the quantum pendulum $E_a < E_b < E_c$, any pair of integers (m_1, m_2) uniquely determines Δ and ω via the coupled equations

$$m_1\omega = E_b - E_a - \Delta,$$

$$m_2\omega = E_c - E_b + \Delta. \tag{11}$$

Eliminating ω we obtain an expression for Δ,

$$\Delta = \frac{m_2\omega_1 - m_1\omega_2}{m_1 + m_2}, \tag{12}$$

where we have defined $\omega_1 = E_b - E_a$ and $\omega_2 = E_c - E_b$. We can see that the integer vectors $\vec{m} \equiv (m_1, m_2)^T$ which minimize Δ are those which satisfy

$$\vec{m}\cdot\vec{\nu} \approx 0 \quad \text{with } \vec{\nu} \equiv (-\omega_2, \omega_1)^T. \tag{13}$$

Therefore, the best choices for $\vec{m}$ are those for which m_1/m_2 are the best rational approximants of the ratio $w \equiv \omega_1/\omega_2$.

Let us denote the unperturbed Floquet Hamiltonian ($\hat{H}_F$ when $\lambda = 0$) as

$$\hat{H}_F^0 \equiv \hat{H}_{\text{pend}} - i\frac{\partial}{\partial t}. \tag{14}$$

In the extended Hilbert space, $\hat{H}_F^0$ has normalized eigenstates of the form

$$\langle t|n,q\rangle \equiv \langle t|q\rangle|\chi_n\rangle = \frac{1}{\sqrt{T}}e^{iq\omega t}|\chi_n\rangle, \quad q \in \mathbb{Z}. \tag{15}$$

The corresponding eigenvalues are $\epsilon_{n,q}^0 = E_n + q\omega$. We are interested in the dynamics of an initial population of atoms localized in the pendulum state $|\chi_a\rangle$. With $\lambda = 0$, state $|\chi_a\rangle$ is represented in a particular zone of Floquet eigenvalues of $\hat{H}_F^0$ by a Floquet eigenstate $|a, q_a\rangle$ with eigenvalue ϵ_{a,q_a} in that zone. The coupling frequencies Ω_1 and Ω_2 have been chosen in Eq. (11) such that ϵ_{c,q_c}^0, the Floquet eigenvalue in that zone corresponding to the physical state $|\chi_c\rangle$, is equal to ϵ_{a,q_a}^0 and the eigenvalue ϵ_{b,q_b}^0 is offset from this value by Δ. The degeneracy of these two eigenvalues and the near degeneracy of the third requires that any perturbation analysis must be performed in the degenerate form [21]. Therefore, we expand the extended Hilbert space state $|\phi\rangle$ in powers of the small parameter λ,

$$|\phi\rangle = |\phi^{(0)}\rangle + \lambda|\phi^{(1)}\rangle + \lambda^2|\phi^{(2)}\rangle + \cdots \tag{16}$$

and take the zeroth-order state to be a superposition of the three degenerate or near-degenerate eigenstates of $\hat{H}_F^0$,

$$|\phi^{(0)}\rangle = C_a|a,q_a\rangle + C_b|b,q_b\rangle + C_c|c,q_c\rangle. \tag{17}$$

The eigenvalue is likewise expanded in orders of the small parameter,

$$\epsilon = \epsilon^{(0)} + \lambda\epsilon^{(1)} + \lambda^2\epsilon^{(2)} + \cdots. \tag{18}$$

For brevity of notation, we write the unperturbed eigenstates $|a\rangle \equiv |a,q_a\rangle$, $|b\rangle \equiv |b,q_b\rangle$, and $|c\rangle \equiv |c,q_c\rangle$, with associated eigenvalues $\epsilon_a^0 \equiv \epsilon_{a,q_a}^0$, $\epsilon_b^0 \equiv \epsilon_{b,q_b}^0$, and $\epsilon_c^0 \equiv \epsilon_{c,q_c}^0$, respectively.

Retaining terms up to first order in λ, we obtain an isolated subsystem of Eq. (10):

$$\begin{pmatrix} \epsilon_a^0 + \lambda V_{a,a} & \lambda V_{a,b} & \lambda V_{a,c} \\ \lambda V_{b,a} & \epsilon_b^0 + \lambda V_{b,b} & \lambda V_{b,c} \\ \lambda V_{c,a} & \lambda V_{c,b} & \epsilon_c^0 + \lambda V_{c,c} \end{pmatrix} \begin{pmatrix} C_a \\ C_b \\ C_c \end{pmatrix} = \epsilon' \begin{pmatrix} C_a \\ C_b \\ C_c \end{pmatrix}, \tag{19}$$

where $\epsilon' \equiv \epsilon_a^0 + \lambda \epsilon^{(1)}$ and we have assumed that Δ is of order λ. The matrix elements of the perturbation are determined in the following way:

$$\begin{aligned} V_{i,j} &= \langle\langle i, q_i | \hat{V} | j, q_j \rangle\rangle \equiv \int_{-\pi/\omega}^{\pi/\omega} \langle q_i | t \rangle \langle t | q_j \rangle \langle \chi_i | \cos \hat{x} | \chi_j \rangle \\ &\quad \times [\kappa_1 \cos(m_1 \omega t) + \kappa_2 \cos(m_2 \omega t)] dt \\ &= \frac{\langle \chi_i | \cos \hat{x} | \chi_j \rangle}{2} (\kappa_1 \delta_{q_j, q_i + m_1} + \kappa_1 \delta_{q_j, q_i - m_1} \\ &\quad + \kappa_2 \delta_{q_j, q_i + m_2} + \kappa_2 \delta_{q_j, q_i - m_2}), \end{aligned} \tag{20}$$

where it is customary to express the inner product in the extended Hilbert space with double brackets. The selection of Ω_1 and Ω_2 guarantees that the q indices for these states satisfy

$$q_b - q_a = m_1 \quad \text{and } q_c - q_b = m_2. \tag{21}$$

Therefore, the only nonzero matrix elements of the perturbation are $V_{a,b} = V_{b,a}$ and $V_{b,c} = V_{c,b}$. Further, we can write

$$V_{a,b} = V_{b,a} = \kappa_1 v_{a,b} \quad \text{and } V_{b,c} = V_{c,b} = \kappa_2 v_{b,c}, \tag{22}$$

where the numerical values of

$$v_{i,j} = \frac{\langle \chi_i | \cos \hat{x} | \chi_j \rangle}{2} \tag{23}$$

are calculated using the Mathieu functions. Subtracting $\epsilon_a^0 (C_a, C_b, C_c)^T$ from both sides of Eq. (19) and redefining $\epsilon' - \epsilon_a^0 \to \epsilon'$, we arrive at

$$\begin{pmatrix} 0 & \lambda \kappa_1 v_{a,b} & 0 \\ \lambda \kappa_1 v_{b,a} & \Delta & \lambda \kappa_2 v_{b,c} \\ 0 & \lambda \kappa_2 v_{b,c} & 0 \end{pmatrix} \begin{pmatrix} C_a \\ C_b \\ C_c \end{pmatrix} = \epsilon' \begin{pmatrix} C_a \\ C_b \\ C_c \end{pmatrix}, \tag{24}$$

which is equivalent to the STIRAP model system. Thus, in the limit of small λ (and Δ), the parameters κ_1 and κ_2 can be adiabatically varied in the manner described in the introduction to affect a transition between the unperturbed states $|a\rangle$ and $|c\rangle$.

We now provide a concrete example on which to demonstrate the analysis. Figure 2(a) shows the energies of the first few eigenstates of $\hat{H}_{\text{pend}}$ as a function of κ_0. Husimi representations [21,22] of the even eigenstates, at $\kappa_0 = 8$, are shown in Fig. 3. At this value of κ_0, we choose energies $E_a = E_0$, $E_b = E_4$, and $E_c = E_6$ for coupling. These energy levels have spacings $\omega_1 = E_b - E_a = 12.566\,839\,5$ and $\omega_2 = E_c - E_b = 3.663\,047\,2$ with ratio

$$w = 3.430\,706\,39\cdots = [3,2,3,9,\ldots] = 3 + \cfrac{1}{2 + \cfrac{1}{3 + \cfrac{1}{9 + \cdots}}}. \tag{25}$$

Thus, the best rational approximants of w, found by truncating the continued fraction, are $\{\frac{3}{1}, \frac{7}{2}, \frac{24}{7}, \frac{223}{65}, \ldots\}$. Using the third approximation, the modulation frequencies shown in the example have been chosen to be $\Omega_1 = 24\omega$ and $\Omega_2 = 7\omega$, giving $\omega = 0.5235$ and $\Delta = 1.766 \times 10^{-3}$.

In Fig. 2(b), the Floquet eigenvalues of H_F^0 are shown in the zone $\epsilon^\star = 0$. In the inset figure, one can see that $\epsilon_a^0 = \epsilon_{0,12}^0$ and $\epsilon_c^0 = \epsilon_{6,-19}^0$ are equal at $\kappa_0 = 8$ and $\epsilon_b^0 = \epsilon_{4,-12}^0$ is offset by Δ. Using the Mathieu functions, the perturbation matrix elements are calculated to be

$$V_{a,b} = V_{b,a} = \kappa_1 v_{a,b} = -1.16 \times 10^{-2} \kappa_1, \tag{26}$$

$$V_{b,c} = V_{c,b} = \kappa_2 v_{b,c} = 2.50 \times 10^{-1} \kappa_2. \tag{27}$$

To accomplish a STIRAP transition from $|a\rangle$ to $|c\rangle$, we give κ_1 and κ_2 Gaussian dependence on an adiabatic time parameter t' [see Fig. 4(a)],

$$\kappa_i(t') = \exp\left(-\frac{(t' - t_i)^2}{2\sigma_i^2}\right). \tag{28}$$

The conditions of Eq. (3) are satisfied by setting $t_1 = -t_2 = 1.0$ and $\sigma_1 = \sigma_2 = 1.0$. Figure 4 shows good agreement between the adiabatic dynamics of the model system in Eq. (24) [Figs. 4(b) and 4(d)] and that of the full Floquet Hamiltonian [Figs. 4(c) and 4(e)].

The implementation of this transition in an experimental system (or the numerical evolution of the Schrödinger equation) is not dependent on the time periodicity which we have required thus far. Floquet analysis has proven to be an essential theoretical tool in revealing the existence of the STIRAP model, but the method has introduced no upper limit on the integers m_1 and m_2 whose ratio approximates ω_1/ω_2. Therefore we may choose the coupling frequencies to be resonant ($\Omega_1 = \omega_1$ and $\Omega_2 = \omega_2$) to any desired accuracy. The results for the numerical evolution of the effective Schrödinger equation in Eq. (8) are shown in Fig. 5(a), for the case of both resonant and near-resonant coupling ($\Delta = 1.77 \times 10^{-3}$) with $\lambda = 0.1$. The evolution was performed over a set time period $[0, t_{\text{tot}}]$ with initial condition $|\langle \chi_a | \psi \rangle|^2 = 1$, and Gaussian parameters for the coupling amplitudes κ_1 and κ_2 of $\sigma_1 = \sigma_2 = 0.1 t_{\text{tot}}$, $t_1 = 0.6 t_{\text{tot}}$, and $t_2 = 0.4 t_{\text{tot}}$. It is seen that resonant coupling provides a more rapid approach to the adiabatic behavior. In Fig. 5(b), good agreement is seen between the resonant evolution of the full effective Schrödinger equation and the adiabatic predictions of Fig. 4(e).

III. STIRAP TRANSITIONS FROM STATIONARY TO MOVING ATOMS

We now consider the case in which the "unperturbed" Hamiltonian has the form of Eq. (4), which consists classi-

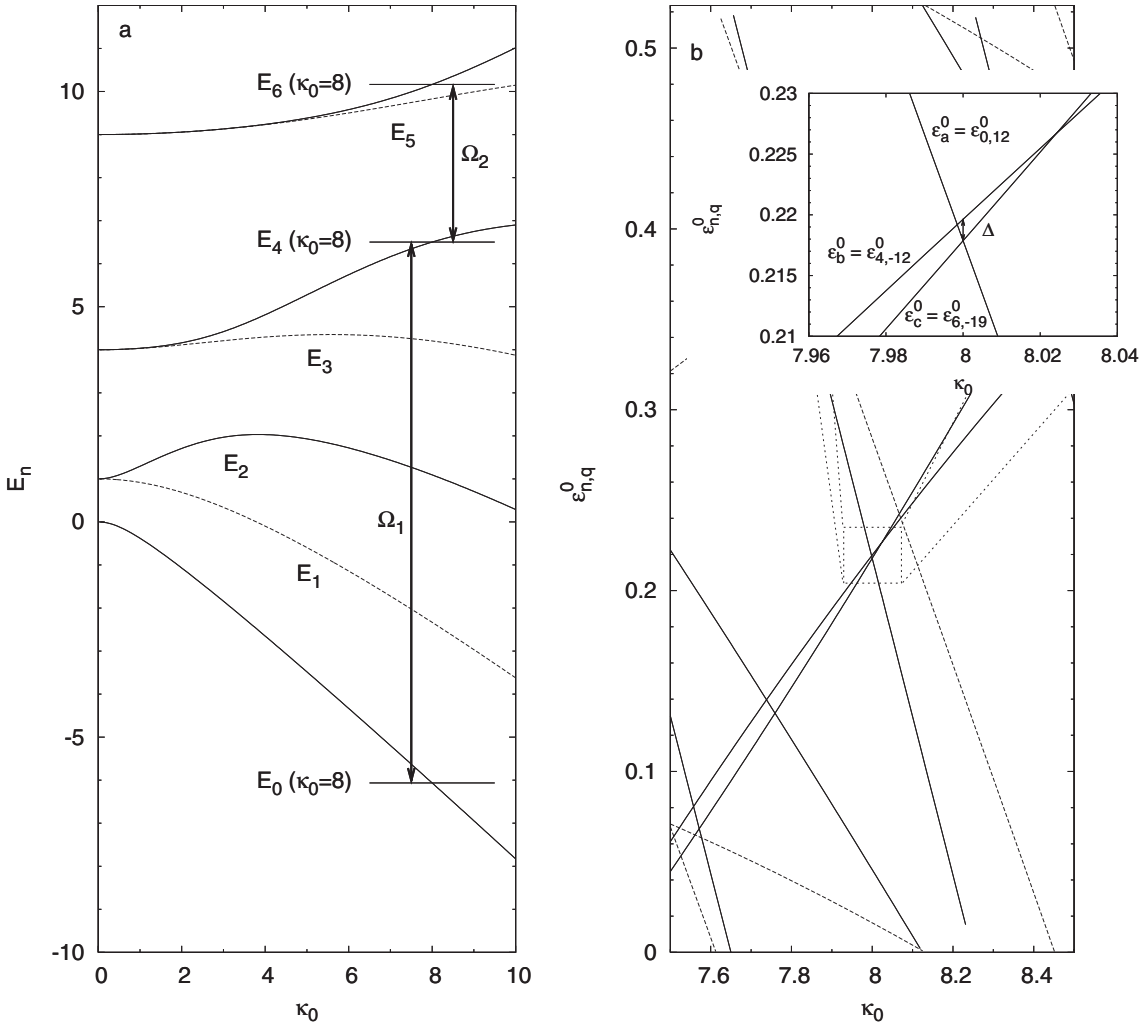

FIG. 2. The lowest seven energies of the quantum pendulum (a) as a function of the parameter κ_0 (solid lines are the energies of even-parity states, dotted odd). The coupling of levels E_0-E_4 and E_4-E_6 at $\kappa_0=8$ via the perturbation $\hat{V}(t)$ requires a Floquet treatment of the pendulum system. The corresponding Floquet eigenvalues (for $\omega=0.5235$) are shown in (b). The degeneracy and near degeneracy of the three coupled eigenvalues can be seen in the enlarged (inset) view.

cally of a stationary cosine wave and a cosine wave that travels through phase space with a speed ω_0. Our goal is to cause a coherent transition of an entire cloud of trapped atoms from a state localized in the stationary wave (in the sense of its Husimi distribution) into a state localized in the traveling wave, so that the entire collection of atoms changes velocity from $v=0$ to $v=\omega_0$.

Our approach is analogous to that of the preceding section. We apply perturbation theory to a Floquet eigensystem of the form

$$\hat{H}_F(t)|\phi(t)\rangle = [\hat{H}_F^0(t) + \lambda \hat{V}(t)]|\phi(t)\rangle = \epsilon|\phi(t)\rangle, \qquad (29)$$

where $\hat{H}_F$ is periodic in time with period $T=2\pi/\omega$ and the perturbation operator $\hat{V}$ has the same form as in Eq. (6). Again we find that, in the limit of small λ, there exists an isolated three-level subsystem in which a STIRAP-type transition between eigenstates of $\hat{H}_F^0$ can be induced. The construction of $\hat{H}_F$, however, differs significantly from the preceding section because of the explicit time dependence of the two-resonance Hamiltonian. In the pendulum analysis, the frequencies Ω_1 and Ω_2 were chosen to couple the energies of pendulum eigenstates. Here, these frequencies are chosen to couple the eigenvalues of the two-resonance Floquet Hamiltonian,

$$\hat{H}_F^0(t) = \hat{p}^2 + \kappa_0[\cos\hat{x} + \cos(\hat{x} - \omega_0 t)] - i\frac{\partial}{\partial t}, \qquad (30)$$

within a particular zone (note that we have redefined $\hat{H}_F^0$ in this section). Selection of coupling frequencies such that they and ω_0 are commensurate allows for Floquet analysis of the full system, but requires that the eigenstates of $\hat{H}_F^0$ be translated from their natural Hilbert space, containing functions periodic in time with period $\bar{T}\equiv 2\pi/\omega_0$, into the space containing T-periodic functions of time. The relevant Floquet eigenvalues associated to the eigenstates in this latter space take near-degenerate values and perturbation analysis leads

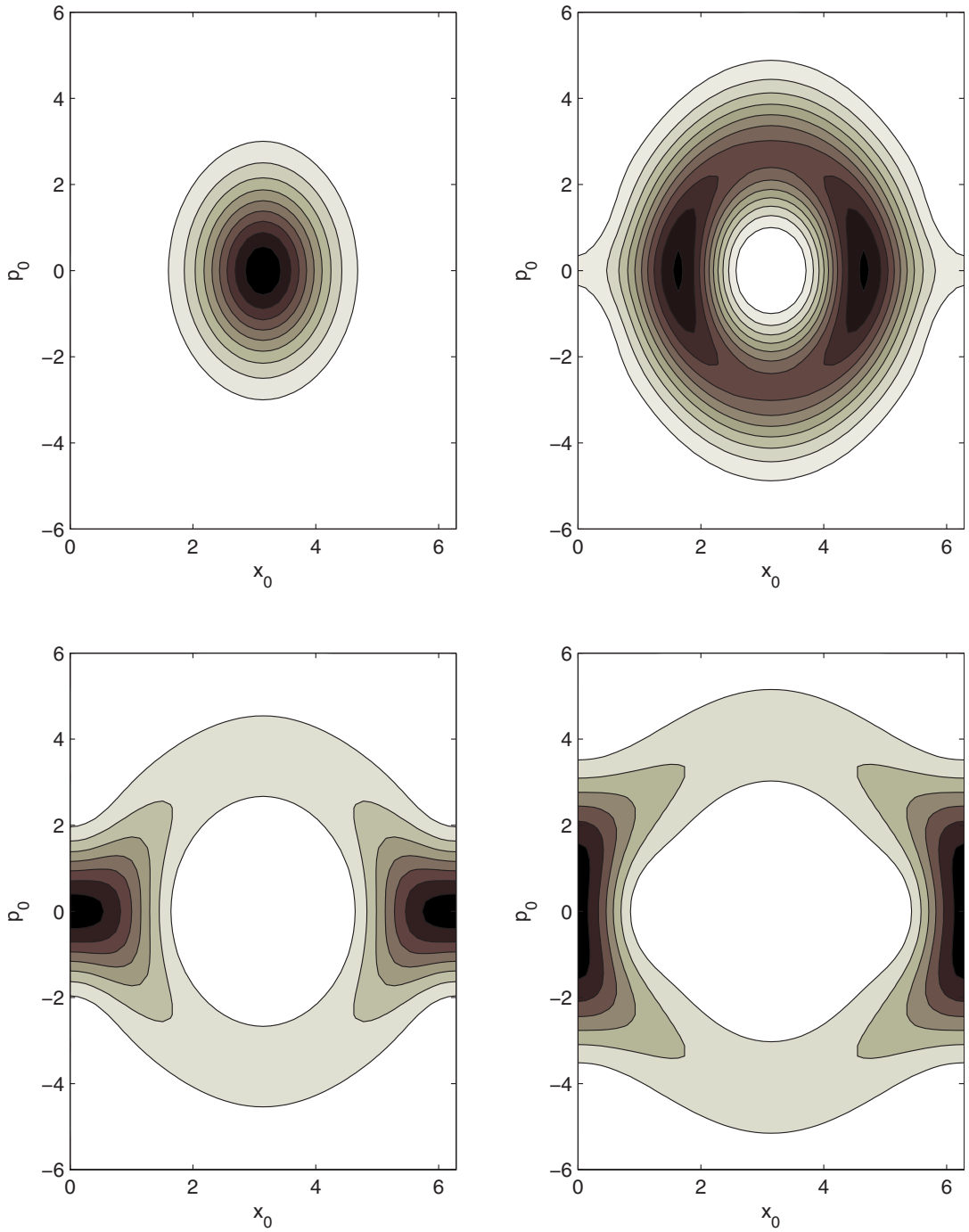

FIG. 3. (Color online) The Husimi functions of the first four even-parity eigenstates of the quantum pendulum on the dimensionless classical phase space coordinates (x_0, p_0). The states are, clockwise from top left, $|\chi_0\rangle, |\chi_2\rangle, |\chi_6\rangle, |\chi_4\rangle$.

to similar results as the preceding section. [It should also be noted that although we call the two-resonance system in Eq. (30) an "unperturbed" Hamiltonian, it is not analytically solvable. Perturbation theory will be a useful tool to demonstrate the existence of a STIRAP-like model for this system, but the eigenstates of $\hat{H}_F^0$ and all related quantities (e.g., the matrix elements of the three-level system) must be determined numerically.]

We begin by constructing Floquet eigenstates $|\bar{\phi}_{\alpha'}^0\rangle$ of $\hat{H}_F^0$ (the "overbar" will be used to indicate that these states belong to the Hilbert space $\bar{\mathcal{H}}$, defined below). We will assume that the parameters κ_0 and ω_0 have constant values, which may be set arbitrarily. The only limitation on this choice is that, given ω_0, κ_0 should be chosen such that the set of eigenstates with eigenvalues in a particular zone contains one state localized purely in the stationary cosine wave and one state localized in the traveling wave (i.e., a κ_0 value far from avoided crossings involving the eigenvalues of these states). The eigenstates $|\bar{\phi}_{\alpha'}^0\rangle$ lie in the extended Hilbert space $\bar{\mathcal{H}} \equiv \Theta \otimes \bar{\mathcal{T}}$, where Θ is the space of all 2π-periodic, square-

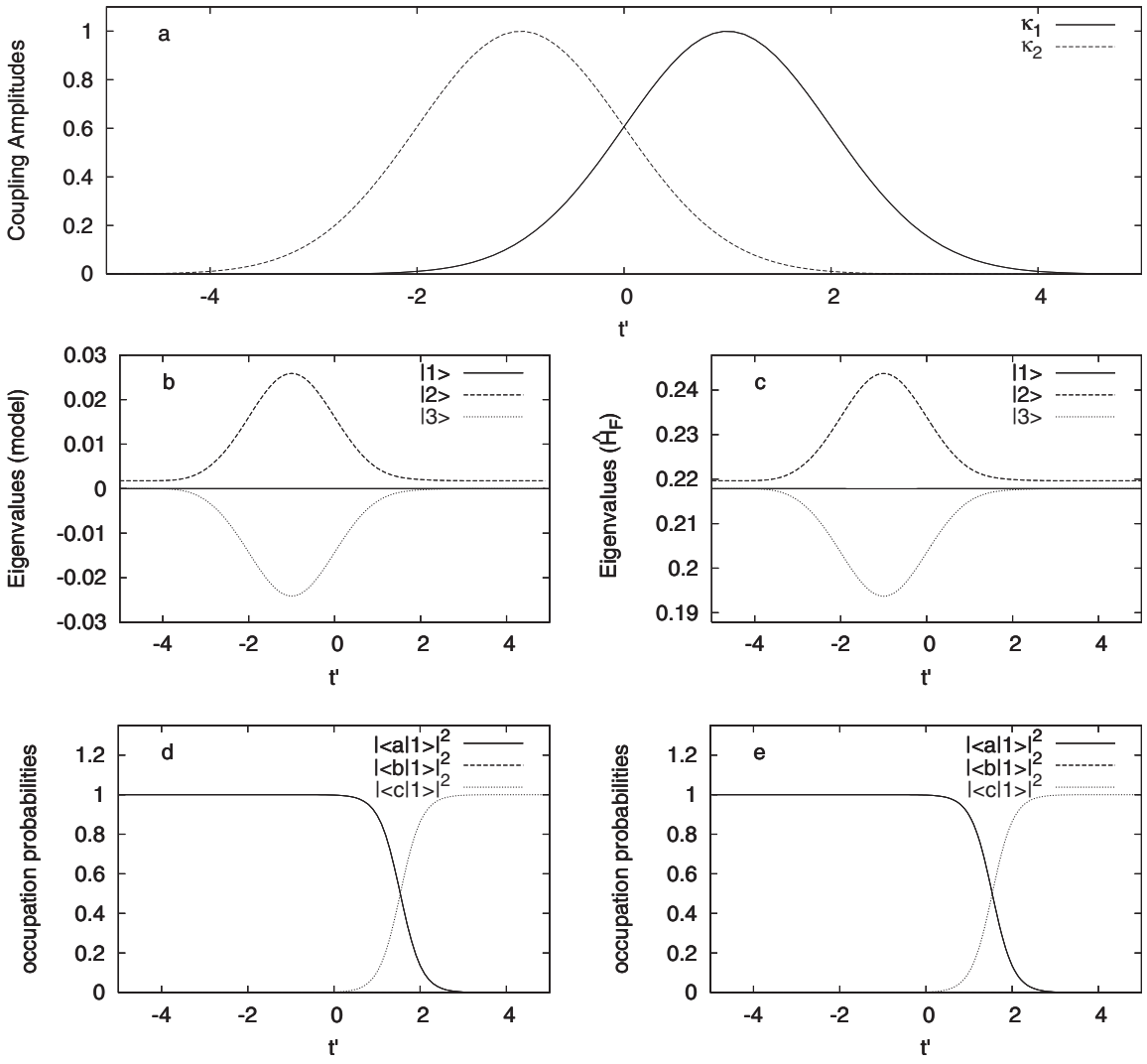

FIG. 4. Adiabatic evolution of the pendulum system under STIRAP coupling, comparing the dynamics of the model in Eq. (24) [(b) and (d)] to that of the full Floquet Hamiltonian in Eq. (8) [(c) and (e)] for $\lambda=0.1$. It is useful to compare this evolution to that of the model system presented in Fig. 1. The coupling field κ_2 is seen to have a greater effect on the eigenvalues at $t'=-1$ than that of κ_1 at $t'=1$, since $|v_{b,c}| \gg |v_{a,b}|$. This asymmetry also shifts the transition of the $|1\rangle$ eigenvector from unperturbed state $|a\rangle$ to $|c\rangle$ to a later time [(d) and (e)]. All plotted quantities are dimensionless functions of the dimensionless parameter t'.

normalizable position-space functions and $\bar{\mathcal{T}}$ is the space of all $\bar{T}$-periodic, square-normalizable functions of time. We select the complete set of momentum eigenvectors $|n\rangle$ (see Appendix A) as a basis in Θ and the analogous eigenvectors $|q\rangle$ as a basis in $\bar{\mathcal{T}}$, yielding normalized basis vectors in the extended space which can be written

$$\langle x,t|n,q\rangle \equiv \langle x|n\rangle\langle t|q\rangle = \frac{1}{\sqrt{2\pi\bar{T}}} e^{inx} e^{iq\omega_0 t}, \tag{31}$$

with $n,q \in \mathbb{Z}$. The eigenstates $|\bar{\phi}^0_\alpha\rangle$ can then be written

$$|\bar{\phi}^0_\alpha(t)\rangle = \sum_{n,q} \frac{1}{\sqrt{\bar{T}}} e^{iq\omega_0 t}\langle n,q|\bar{\phi}^0_\alpha\rangle|n\rangle, \tag{32}$$

where $|\bar{\phi}^0_\alpha(t)\rangle = \langle t|\bar{\phi}^0_\alpha\rangle$ and the coefficients $\langle n,q|\bar{\phi}^0_\alpha\rangle$ are determined by diagonalization of $\hat{H}^0_F$ in $\bar{\mathcal{H}}$.

We select a zone $\epsilon^\star \leqslant \bar{\epsilon}^0_\alpha < \epsilon^\star + \omega_0$ within which to perform a coupling of the eigenvalues $\bar{\epsilon}^0_\alpha$ of $\hat{H}^0_F$. Two of these eigenvalues, which we denote $\bar{\epsilon}^0_a$ and $\bar{\epsilon}^0_c$, correspond to eigenstates localized in the stationary and traveling waves, respectively. A third eigenvalue $\bar{\epsilon}^0_b$ is chosen with the restriction that the corresponding eigenstate is localized "nearby" in phase space (the matrix element of $\cos\hat{x}$ between this and the other two states should not be vanishingly small). As before, the coupling frequencies Ω_1 and Ω_2 must be chosen to be commensurate. In this case, however, analogous equations to Eqs. (11) cannot be solved simultaneously with the requirement that ω_0 is likewise commensurate,

$$\omega_0 = m_0\omega \quad (m_0 \in \mathbb{Z}). \tag{33}$$

Therefore, in the following, we will relax the equal detuning requirement and allow for two independent detunings defined by the equations

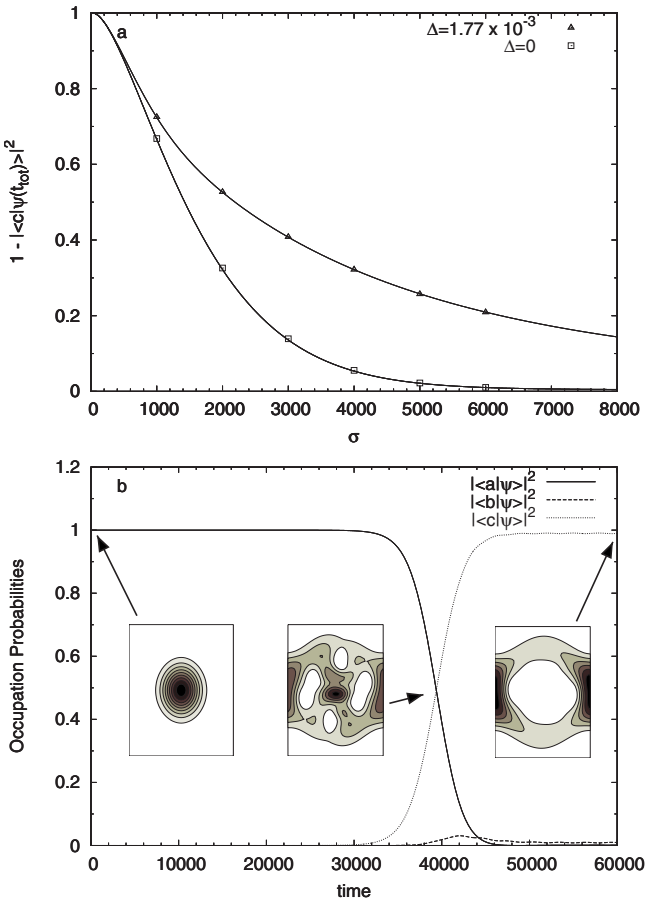

FIG. 5. (Color online) The numerical evolution of a state initially localized in the $|\chi_a\rangle$ pendulum state ($|\langle\chi_a|\psi(t=0)\rangle|^2=1$), under STIRAP coupling of the energies. The probability of a nonadiabatic transition (transition to any state other than $|c\rangle$ in time $t=t_{\text{tot}}$) is plotted versus the width of the Gaussian fields $\sigma=\sigma_1=\sigma_2=0.1t_{\text{tot}}$ (a). The coupling strength was fixed at $\lambda=0.1$ with maximum values of the two fields for a particular realization occurring at $t_1=0.6t_{\text{tot}}$ and $t_2=0.4t_{\text{tot}}$. The approach to adiabaticity for the evolution of the effective Schrödinger equation is seen to be more rapid in the case of resonant coupling (squares) than for near-resonant coupling (triangles); solid lines show the evolution predicted by the three-state model. (b) shows the full numerical evolution under the Schrödinger equation corresponding to the point at $\sigma=6000$ with resonant ($\Delta=0$) coupling in (a). A state classically localized within the pendulum well transitions to one localized on the separatrix (axes on inset Husimi functions are the same as in Fig. 3). The horizontal axes of both plots are dimensionless time measured in units of $\frac{1}{4\omega_r}$.

$$\Omega_1 = m_1\omega = (\bar{\epsilon}_b^0 - \bar{\epsilon}_a^0) - \Delta_1,$$

$$\Omega_2 = m_2\omega = (\bar{\epsilon}_c^0 - \bar{\epsilon}_b^0) + \Delta_2. \tag{34}$$

Given any integer vector $\vec{m}\equiv(m_0,m_1,m_2)^T$, Eqs. (33) and (34) can be solved for $(\Delta_1,\Delta_2,\omega)$. Eliminating ω and defining $\omega_1\equiv\bar{\epsilon}_b^0-\bar{\epsilon}_a^0$ and $\omega_2\equiv\bar{\epsilon}_c^0-\bar{\epsilon}_b^0$, we obtain

$$\Delta_1 = \frac{m_0\omega_1 - m_1\omega_0}{m_0},$$

$$\Delta_2 = \frac{m_2\omega_0 - m_0\omega_2}{m_0}. \tag{35}$$

Thus, we see that the integer vectors $\vec{m}$ which simultaneously minimize the two detunings will be those closest to the vector perpendicular to the plane defined by $\vec{\nu}^{(1)}\equiv(\omega_1,-\omega_0,0)^T$ and $\vec{\nu}^{(2)}\equiv(-\omega_2,0,\omega_0)^T$. This perpendicular vector is of course $\vec{n}=(\omega_0,\omega_1,\omega_2)^T$, and the problem of minimizing the detunings is reduced to finding the best integer approximate of $\vec{n}$ or, equivalently, finding the simultaneous pair of rational approximants for $(\omega_1/\omega_0,\omega_2/\omega_0)$.

In the context of the three-level model system presented in the introduction, nonequal detuning of the coupling frequencies leads to a Hamiltonian of the form

$$H = -\frac{\hbar}{2}\begin{pmatrix} 0 & W_1 & 0 \\ W_1 & -2\Delta_1 & W_2 \\ 0 & W_2 & \Delta_2-\Delta_1 \end{pmatrix}. \tag{36}$$

It was recognized by Kuklinski *et al.* [12] that this system could allow for a STIRAP transition, despite the absence of an analytical result analogous to Eqs. (2) and (3), as long as the condition $\sqrt{W_1^2+W_2^2}\gg|\Delta_2-\Delta_1|$ is satisfied. In order to satisfy this requirement, and that of small perturbations, we will seek integer vectors $\vec{m}$ which provide detunings $|\Delta_2-\Delta_1|\ll|\Delta_1|\ll 1$.

Since the full, perturbed system $\hat{H}_F(t)$ is periodic in time with period $T\equiv 2\pi/\omega$, we must determine the eigenstates of the unperturbed Floquet Hamiltonian in the extended Hilbert space $\mathcal{H}\equiv\Theta\otimes\mathcal{T}$, where $\mathcal{T}$ is the Hilbert space of T-periodic functions. These eigenstates $|\phi_\alpha^0\rangle$ can be expanded in $\mathcal{H}$ as

$$|\phi_\alpha^0(t)\rangle = \sum_{n,q}\frac{1}{\sqrt{T}}e^{iq\omega t}\langle n,q|\phi_\alpha^0\rangle|n\rangle, \tag{37}$$

where the basis vectors $\langle t|q\rangle$ now have the time periodicity of $\mathcal{T}$. Since the Schrödinger equation for the unperturbed system

$$i\frac{\partial}{\partial t}|\psi(t)\rangle = \{\hat{p}^2+\kappa_0[\cos\hat{x}+\cos(\hat{x}-\omega_0 t)]\}|\psi(t)\rangle \tag{38}$$

can be viewed as time periodic with either period $\bar{T}$ or $T=m_0\bar{T}$, a physical solution $|\psi_\alpha(t)\rangle$ can be written, using Eq. (9), in terms of a Floquet state with either periodicity. Equating these two representations, we obtain a relationship between the Floquet eigenstates of $\hat{H}_F^0$ in spaces $\bar{\mathcal{H}}$ and $\mathcal{H}$,

$$\exp(-i\bar{\epsilon}_\alpha^0 t)|\bar{\phi}_\alpha^0(t)\rangle = A\exp(-i\epsilon_\alpha^0 t)|\phi_\alpha^0(t)\rangle, \tag{39}$$

where ϵ_α^0 is the eigenvalue associated to $|\phi_\alpha^0(t)\rangle$ and A is a proportionality constant. Equating coefficients of the momentum eigenvector $|n\rangle$ in Eqs. (32) and (37), we find

$$\sum_q \exp(iqm_0\omega t)\langle n,q|\bar{\phi}_\alpha^0\rangle = \sum_{q'} A'\exp[i(q'\omega-\epsilon_\alpha^0+\bar{\epsilon}_\alpha^0)t]\langle n,q'|\phi_\alpha^0\rangle, \tag{40}$$

where A' is again a constant. A nontrivial solution to this

equation requires that the eigenvalues satisfy $\epsilon^0_\alpha - \bar{\epsilon}^0_\alpha = Q\omega$, where Q is an integer. We see, then, that associated to each Floquet eigenstate in $\bar{\mathcal{H}}$ is a family of eigenstates in $\mathcal{H}$,

$$\{|\phi^0_{\alpha,Q}\rangle, \epsilon^0_{\alpha,Q}\}, \quad Q \in \mathbb{Z}, \tag{41}$$

with $\epsilon^0_{\alpha,Q} = \bar{\epsilon}^0_\alpha + Q\omega$. Selecting a particular value of Q, Eq. (40) becomes

$$\sum_q \exp(iqm_0\omega t)\langle n,q|\bar{\phi}^0_\alpha\rangle = \sum_{q'} A' \exp[i(q'-Q)\omega t]\langle n,q'|\phi^0_{\alpha,Q}\rangle. \tag{42}$$

Equating coefficients of the exponentials, we find

$$\langle n,q|\phi^0_{\alpha,Q}\rangle = \begin{cases} \left\langle n, \dfrac{q-Q}{m_0}|\bar{\phi}^0_\alpha \right\rangle & \text{when } \dfrac{q-Q}{m_0} \in Z, \\ 0 & \text{otherwise}, \end{cases} \tag{43}$$

where we have set $A'=1$ under normalization. Therefore we see that the unperturbed eigenstates in the space $\mathcal{H}$ have nonzero coefficients $\langle n,q|\phi^0_{\alpha,Q}\rangle$ only at m_0-separated values of q, with an offset of Q from $q=0$.

Within a particular zone, we denote the unbarred eigenvalues corresponding to $\{\bar{\epsilon}^0_a, \bar{\epsilon}^0_b, \bar{\epsilon}^0_c\}$ as $\{\epsilon^0_{a,Q_a}, \epsilon^0_{b,Q_b}, \epsilon^0_{c,Q_c}\}$, with values related by

$$\epsilon^0_{b,Q_b} - \epsilon^0_{a,Q_a} = \Delta_1,$$

$$\epsilon^0_{b,Q_b} - \epsilon^0_{c,Q_c} = \Delta_2, \tag{44}$$

and the corresponding eigenstates $\{|\phi^0_{a,Q_a}\rangle, |\phi^0_{b,Q_b}\rangle, |\phi^0_{c,Q_c}\rangle\}$. The Q indices of these states are related by $Q_a - Q_b = m_1$ and $Q_b - Q_c = m_2$.

Perturbation analysis of Eq. (29) is now performed by expanding the eigenstate $|\phi\rangle$ and eigenvalue ϵ in powers of λ. Assuming that $|\phi^0_{a,Q_a}\rangle$ is initially occupied with probability one, and taking into account the near-degeneracies of Eq. (44), the zeroth-order term in the expansion of the perturbed eigenstate is chosen to be of the form

$$|\phi^{(0)}\rangle = C_a|\phi^0_{a,Q_a}\rangle + C_b|\phi^0_{b,Q_b}\rangle + C_c|\phi^0_{c,Q_c}\rangle. \tag{45}$$

Retaining terms up to first order in λ and making the assumption that Δ_1 and Δ_2 are of order λ, we obtain

$$\begin{pmatrix} \epsilon^0_a + \lambda V_{a,a} & \lambda V_{a,b} & \lambda V_{a,c} \\ \lambda V_{b,a} & \epsilon^0_b + \lambda V_{b,b} & \lambda V_{b,c} \\ \lambda V_{c,a} & \lambda V_{c,b} & \epsilon^0_c + \lambda V_{c,c} \end{pmatrix} \begin{pmatrix} C_a \\ C_b \\ C_c \end{pmatrix} = \epsilon' \begin{pmatrix} C_a \\ C_b \\ C_c \end{pmatrix}, \tag{46}$$

where $\epsilon' \equiv \epsilon^0_a + \lambda\epsilon^{(1)}$ and the matrix elements are calculated, defining $|i\rangle \equiv |\phi^0_{i,Q_i}\rangle$, as follows:

$$\begin{aligned} V_{i,j} \equiv \langle\langle i|\hat{V}|j\rangle\rangle &= \sum_{n,q,n',q'} (\langle i|n,q\rangle\langle n|\cos\hat{x}|n'\rangle\langle n',q'|j\rangle) \\ &\quad \times [\kappa_1\langle q|\cos(m_1\omega\hat{t})|q'\rangle + \kappa_2\langle q|\cos(m_2\omega\hat{t})|q'\rangle] \\ &= \frac{1}{2}\sum_{n,q,n'} \kappa_1\langle n|\cos\hat{x}|n'\rangle(\langle i|n,q\rangle\langle n',q+m_1|j\rangle \\ &\quad + \langle i|n,q\rangle\langle n'q-m_1|j\rangle) \\ &\quad + \kappa_2\langle n|\cos\hat{x}|n'\rangle(\langle i|n,q\rangle\langle n',q+m_2|j\rangle \\ &\quad + \langle i|n,q\rangle\langle n',q-m_2|j\rangle). \end{aligned} \tag{47}$$

Recalling the structure of the states $|\phi^0_{i,Q_i}\rangle$ given in Eq. (43), we see that the sum

$$\sum_q \langle i|n,q\rangle\langle n',q+m|j\rangle = \sum_q \langle\phi^0_{i,Q_i}|n,q\rangle\langle n',q+m|\phi^0_{j,Q_j}\rangle, \tag{48}$$

can be nonzero only when $Q_j + m = Q_i + km_0$ with $k \in Z$. Thus, the only nonzero matrix elements of $\hat{V}$ in Eq. (46) are

$$\begin{aligned} V_{a,b} &= \frac{\kappa_1}{4}\sum_{n,q} (\langle a|n,q\rangle\langle n+1,q-m_1|b\rangle \\ &\quad + \langle a|n,q\rangle\langle n-1,q-m_1|b\rangle) \\ &= \frac{\kappa_1}{4}\sum_{n,q} (\langle\bar{\phi}^0_a|n,q\rangle\langle n+1,q|\bar{\phi}^0_b\rangle + \langle\bar{\phi}^0_a|n,q\rangle\langle n-1,q|\bar{\phi}^0_b\rangle) \\ &= \kappa_1\frac{\langle\langle\bar{\phi}^0_a|(\cos\hat{x}\otimes\mathbb{I})|\bar{\phi}^0_b\rangle\rangle}{2} \end{aligned} \tag{49}$$

and

$$\begin{aligned} V_{b,c} &= \frac{\kappa_2}{4}\sum_{n,q} (\langle b|n,q\rangle\langle n+1,q-m_2|c\rangle \\ &\quad + \langle b|n,q\rangle\langle n-1,q-m_2|c\rangle) \\ &= \frac{\kappa_2}{4}\sum_{n,q} (\langle\bar{\phi}^0_b|n,q\rangle\langle n+1,q|\bar{\phi}^0_c\rangle + \langle\bar{\phi}^0_b|n,q\rangle\langle n-1,q|\bar{\phi}^0_c\rangle) \\ &= \kappa_2\frac{\langle\langle\bar{\phi}^0_b|(\cos\hat{x}\otimes\mathbb{I})|\bar{\phi}^0_c\rangle\rangle}{2}, \end{aligned} \tag{50}$$

where the second and third equalities for each matrix element have been written in terms of the Floquet states in $\bar{\mathcal{H}}$, using Eq. (43). Subtracting $\epsilon^0_a(C_a, C_b, C_c)^T$ from both sides, redefining $\epsilon' - \epsilon^0_a \to \epsilon'$, and defining $v_{a,b} = V_{a,b}/\kappa_1$ and $v_{b,c} = V_{b,c}/\kappa_2$, Eq. (46) becomes

$$\begin{pmatrix} 0 & \lambda\kappa_1 v_{a,b} & 0 \\ \lambda\kappa_1 v_{b,a} & \Delta_1 & \lambda\kappa_2 v_{b,c} \\ 0 & \lambda\kappa_2 v_{c,b} & \Delta_1 - \Delta_2 \end{pmatrix} \begin{pmatrix} C_a \\ C_b \\ C_c \end{pmatrix} = \epsilon' \begin{pmatrix} C_a \\ C_b \\ C_c \end{pmatrix}, \tag{51}$$

which is equivalent to the desired model system in Eq. (36).

Again, we provide an example system on which to demonstrate the analysis. Figure 6(a) shows some eigenvalues $\bar{\epsilon}^0_\alpha$ of the two-resonance Floquet Hamiltonian, in the zone labeled by $\epsilon^\star = -\omega_0/2$ with $\omega_0 = 6.180\,339\,887$, plotted as func-

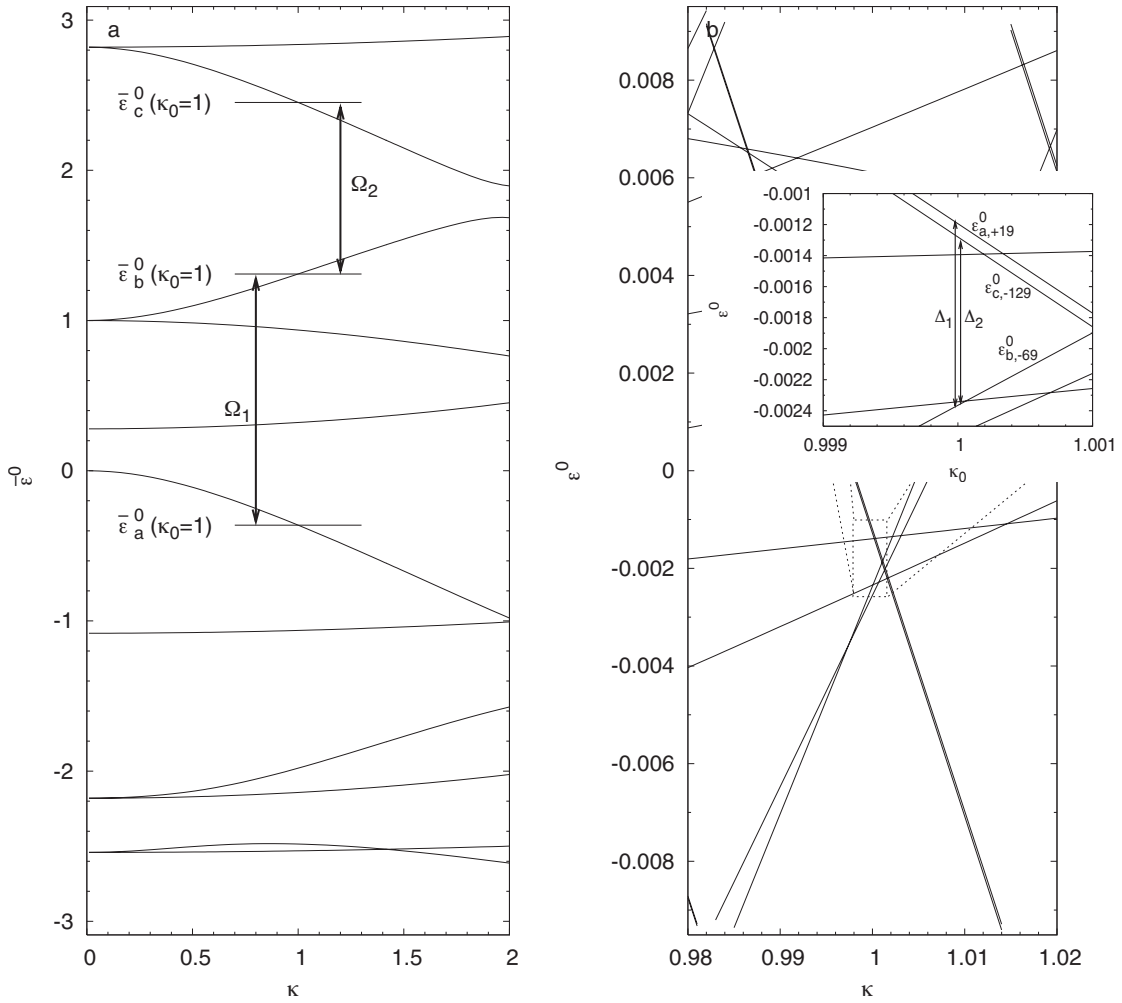

FIG. 6. Eleven eigenvalues of the two-resonance Floquet Hamiltonian with $\omega_0 \approx 6.18$, viewed as an operator in $\bar{\mathcal{H}}$, plotted as a function of κ_0 (a). The corresponding "unbarred" Floquet eigenvalues of the same Hamiltonian, viewed as an operator in the space $\mathcal{H}$ with $\omega = \omega_0/325$, are shown in the zone labeled by $\epsilon^\star = -\omega/2$ (b). The near degeneracy of three eigenvalues ϵ^0_{a,Q_a}, ϵ^0_{b,Q_b}, and ϵ^0_{c,Q_c} at $\kappa_0 = 1$ can be seen in the inset. It is evident that there are other eigenvalues nearly degenerate with these three, however these need not be considered in Eq. (45) since their respective Q values will yield zero-valued matrix elements.

tions of κ_0. A triplet of eigenvalues $\bar{\epsilon}^0_a < \bar{\epsilon}^0_b < \bar{\epsilon}^0_c$ has been chosen at $\kappa_0 = 1$ for STIRAP coupling. The Husimi functions of the three corresponding eigenstates are shown in Fig. 7, where it can be seen that state $|a\rangle$ is localized in the stationary optical lattice at $p_0 = 0$ and state $|c\rangle$ is localized in the traveling lattice at $p_0 = \omega_0/2$. The values of the three eigenvalues satisfy $\omega_1 = \bar{\epsilon}^0_b - \bar{\epsilon}^0_a = 1.672\,274\,95$ and $\omega_2 = \bar{\epsilon}^0_c - \bar{\epsilon}^0_b = 1.142\,070\,65$. Therefore we seek simultaneous rational approximants $(m_1/m_0, m_2/m_0)$ to the pair $(0.270\,579\,771, 0.184\,790\,913)$. Performing a numerical exhaustive search, we find that the integer vector $\vec{m} = (325, 88, 60)$ provides detunings $\Delta_1 = -1.17 \times 10^{-3}$ and $\Delta_2 = -1.08 \times 10^{-3}$, which satisfy the required conditions of $|\Delta_1| = O(\lambda) \ll 1$ and $|\Delta_1 - \Delta_2| \ll \lambda$. The unbarred eigenvalues in the zone $\epsilon^\star = -\omega/2 = -\omega_0/(2 \times 325)$ are shown in Fig. 6(b). The detunings Δ_1 and Δ_2 can be seen in the enlarged section of the graph (inset), separating $\epsilon^0_{b,-69}$ from $\epsilon^0_{a,19}$ and $\epsilon^0_{c,-129}$, respectively. The coefficients

$$v_{a,b} = \frac{0.4442}{2}, \tag{52}$$

$$v_{b,c} = \frac{-0.0673}{2}, \tag{53}$$

are calculated using Eqs. (49) and (50) after numerical diagonalization of $\hat{H}^0_F$ in $\bar{\mathcal{H}}$.

The adiabatic dynamics of the model system in Eq. (51) and the full system in Eq. (29) are shown in Fig. 8, using the same parametrization of the κ_i as in Eq. (28) and $\lambda = 0.02$. Although good agreement is seen between the two, it is evident that the STIRAP transition between eigenstates $|a\rangle$ and $|c\rangle$ is not achieved in either case. The reason for this failure is a narrow avoided crossing at $t' \approx -2.5$ between the eigenvalues of adiabatic states $|1\rangle$ and $|3\rangle$ [see inset of Fig. 8(a)], which affects a transition between unperturbed states $|a\rangle$ and

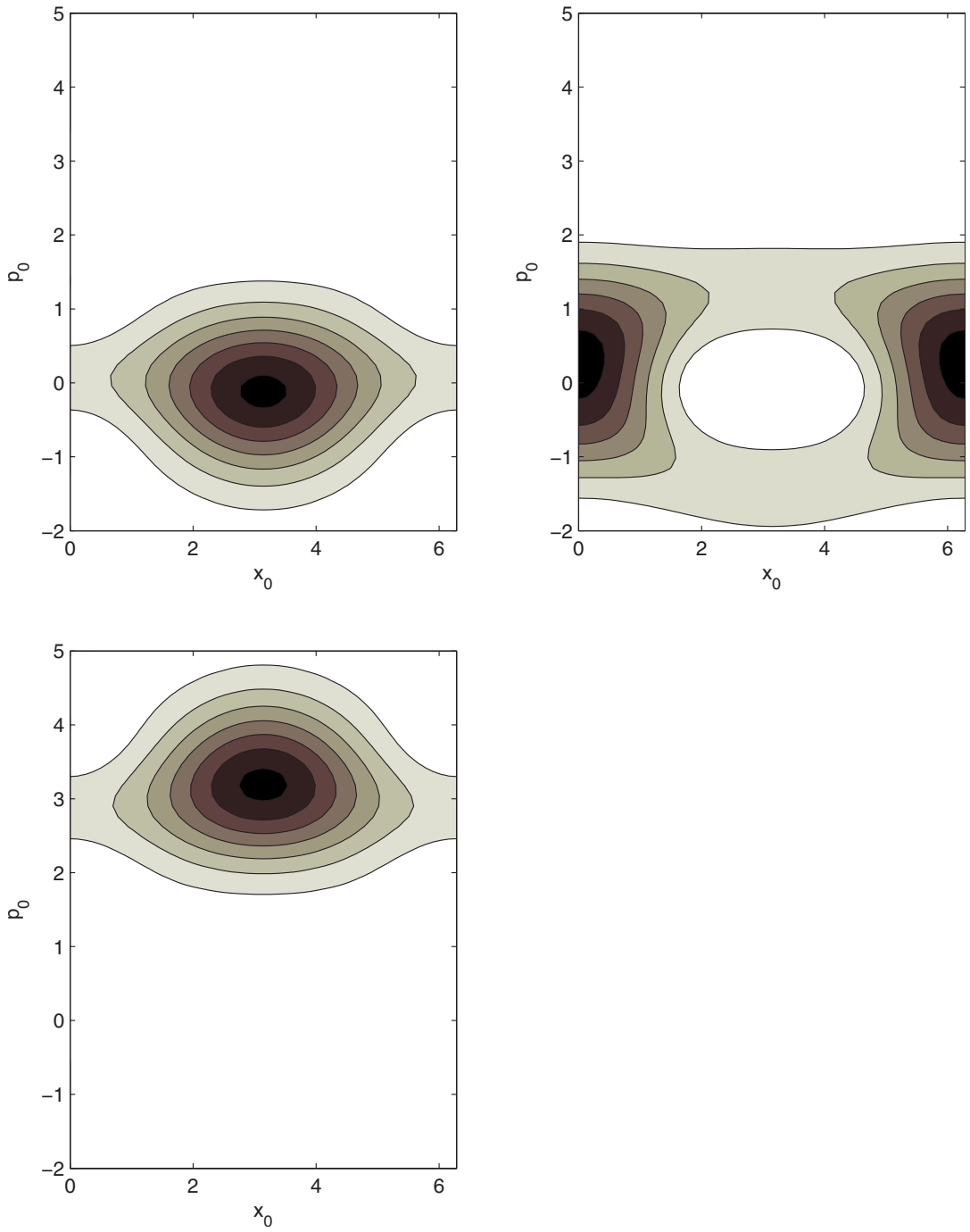

FIG. 7. (Color online) The Husimi representations of three Floquet states of the two-resonance Hamiltonian [$|\bar{\phi}_a^0(t)\rangle$, $|\bar{\phi}_b^0(t)\rangle$, and $|\bar{\phi}_c^0(t)\rangle$, clockwise from top left] viewed at time $t=0$. The parameter values are $\kappa_0=1$ and $\omega_0\approx 6.18$.

$|c\rangle$ *before* the STIRAP transition. This type of avoided crossing, reversing the effects of the desired transition, will always exist in the adiabatic limit when a matrix of the type given in Eq. (36) is used for STIRAP evolution because of the nondegeneracy of the eigenvalues of $|a\rangle$ and $|c\rangle$. Although this model does allow for a broad STIRAP-type transition, the resulting change in character of the adiabatic state $|1\rangle$ as t' passes from $-\infty$ to ∞ requires that its eigenvalue change from 0 to $\Delta_1-\Delta_2$.

The problem in the adiabatic limit can be avoided in the numerical or experimental achievement of a STIRAP transition in one of two ways. First, it is possible to achieve a nonadiabatic evolution of the system which is slow enough to guarantee a STIRAP transition, but rapid enough to pass through problematic sharp avoided crossing via Landau-Zener tunneling. Second, one can abandon time periodicity and apply resonant coupling fields, reducing the model to the classic form in Eq. (1). The efficacy of both methods can be seen in Fig. 9(a), where time evolution of both the model (see Appendix B) and the full Schrödinger equation yield a STIRAP-like transition in the cases of resonant and detuned coupling fields. As in the pendulum case, the resonant cou-

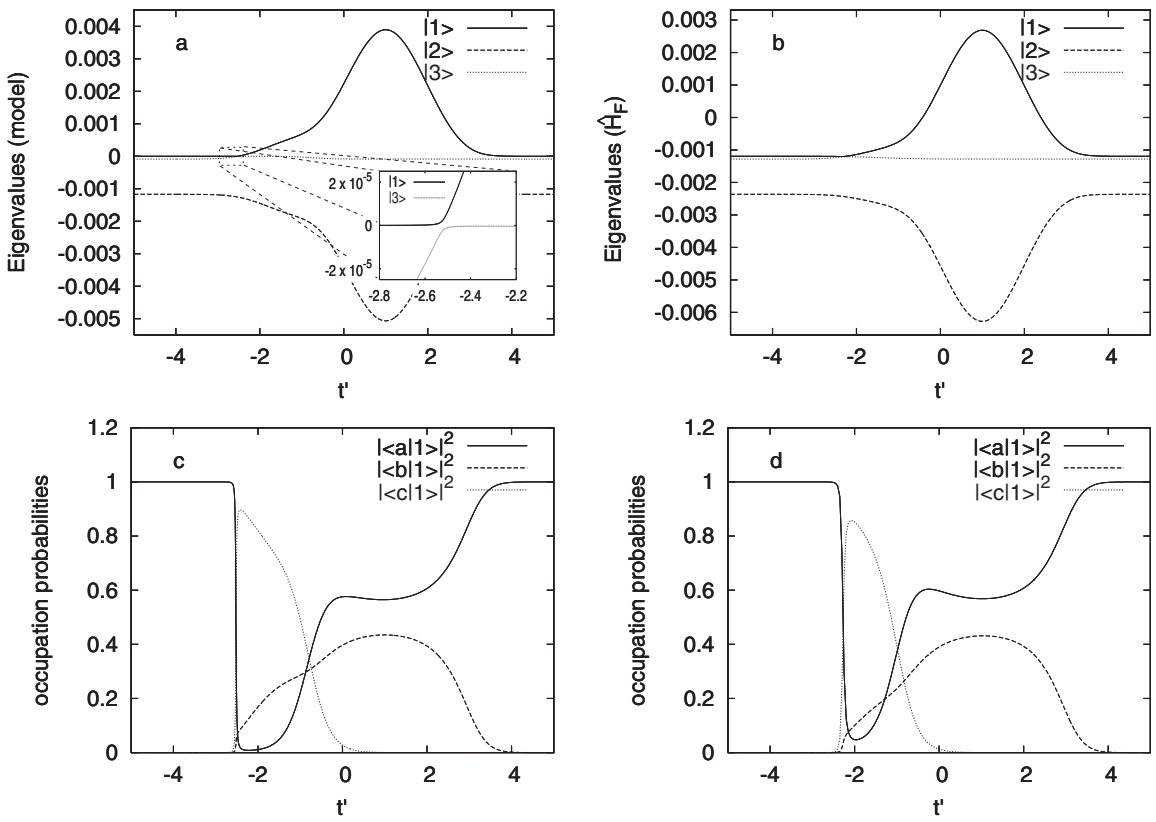

FIG. 8. The adiabatic dynamics of the three-level model in Eq. (51) [(a) and (c)] and the three relevant states of the corresponding full two-resonance Floquet system with $\omega_0 \approx 6.18$ [(b) and (d)] for the example at $\kappa_0 = 1$. The perturbation amplitude functions $\kappa_1(t')$ and $\kappa_2(t')$ are the same as in Fig. 4(a), and $\lambda = 0.02$; model parameters are as determined in the text. The eigenvalues under the application of the perturbation are shown in (a) and (b). The influence of $\kappa_1(t')$ on the adiabatic eigenvalues is stronger than that of $\kappa_2(t')$ because $|v_{a,b}| > |v_{b,c}|$. Overlaps of the $|1\rangle$ adiabatic eigenvector with the unperturbed states are shown in (c) and (d). The inset in (a) shows a sharp avoided crossing which prohibits the STIRAP-like transition in the adiabatic limit. All plotted quantities are dimensionless functions of the dimensionless parameter t'.

pling provides a faster approach to adiabaticity. The evolution of a state initially prepared in the stationary wave eigenstate $|a\rangle$ is shown to pass into the traveling wave state $|c\rangle$ under resonant coupling in Fig. 9(b).

Using the nondimensionalization presented at the end of Appendix A, we can return to physical variables and determine the experimental conditions necessary for a STIRAP transition of the type described here. Consider a system of cold cesium atoms interacting with a system of lasers tuned near the D_2 transition (as in Refs. [23,24]), yielding a recoil frequency of $\omega_r \approx 1.3 \times 10^4$ Hz. For the example considered above, the traveling cosine wave is therefore generated by counterpropagating lasers with frequencies offset by $\delta\omega/2\pi = (4\omega_r)\omega_0/2\pi \approx 51$ kHz; amplitude modulation frequencies corresponding to $\Omega_1/2\pi$ and $\Omega_2/2\pi$ are 14 and 9.4 kHz, respectively. The relationship between dimensionless time t and physical time t_{phys} for this system is

$$t_{\text{phys}} = \frac{t}{4\omega_r} \approx (2 \times 10^{-5}\ \text{s})t. \tag{54}$$

Therefore, the near-100% transition between the stationary and traveling lattices shown in Fig. 9(b) would require 1 s in the laboratory. In this particular example, atoms acquire six recoil momenta which for cesium atoms corresponds to a velocity of 2 cm/s. A more rapid approach to adiabatic evolution can be achieved by increasing the coupling strength λ, as long as the assumption of small perturbation ($\lambda \ll \kappa_0$) remains valid. In numerical experiments, we were able to decrease the transfer time for the preceding example (with resonant coupling) by a factor of 5, while maintaining 90% efficiency, by setting $\lambda \approx 0.1$. Selection of a larger value of κ_0, i.e., deeper wells in the optical lattice, would allow for a larger value of λ and shorter transfer times.

IV. CONCLUSIONS

We have demonstrated a method for the coherent transfer of ultracold atoms from the well of a stationary optical lattice into that of a traveling lattice. The effective Hamiltonian for an atom in such a lattice, constructed by adiabatic elimination of the internal electronic structure, provides a system of eigenstates which determine the center-of-mass dynamics of the atom. We have shown that small, harmonic modulations of the lattice amplitude can allow for a STIRAP-type subsystem of the Schrödinger equation for this effective Hamiltonian, with which transitions between these eigenstates can be induced.

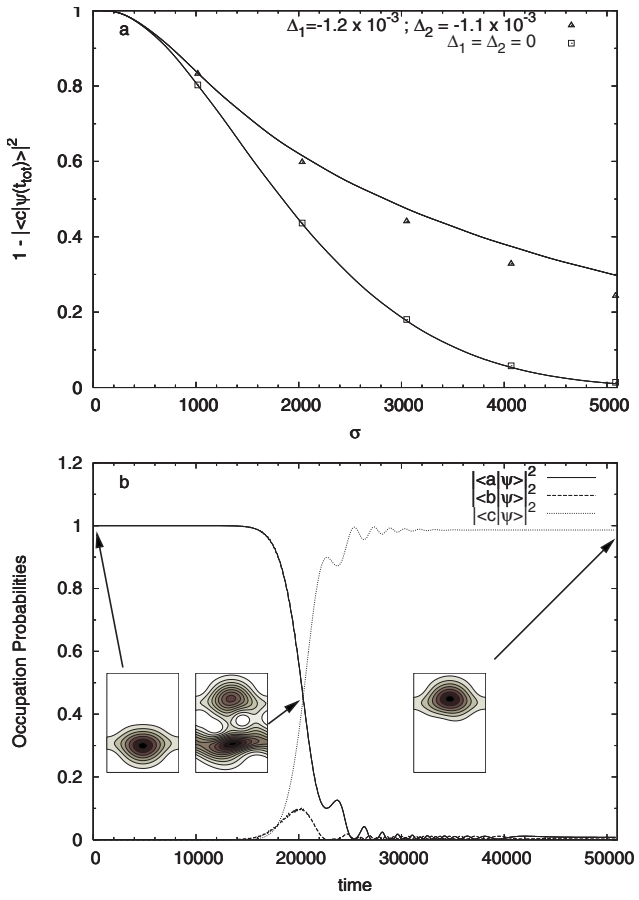

FIG. 9. (Color online) The numerical evolution of a state initially localized in the stationary cosine wave of the two-resonance system $[|\langle\phi_a^0(0)|\psi(0)\rangle|^2=1]$, under the influence of STIRAP coupling for the example described in the text. The probability of a transition to any state other than $|c\rangle$ in time $t=t_{\rm tot}$ is plotted versus the width of the coupling fields $\sigma=\sigma_1=\sigma_2=0.1t_{\rm tot}$ (a). The coupling strength was fixed at $\lambda=0.02$ with maximum values of the two fields for a particular realization occurring at $t_1=0.6t_{\rm tot}$ and $t_2=0.4t_{\rm tot}$. Evolution of the effective Schrödinger equation under resonant coupling is plotted with squares and evolution under near-resonant coupling (with Δ_1 and Δ_2 as shown in Fig. 6) is plotted with triangles. Solid lines are the corresponding values predicted by the numerical evolution of the three-state model. (b) shows the full numerical evolution of the occupation probabilities for the case of $\sigma\approx 5100$ and resonant coupling. A transition from the stationary to traveling lattice is evident in the Husimi representation of the evolved state (axes on inset figures, each taken at an integer multiple of the period $\bar{T}$, are the same as in Fig. 7). The horizontal axes of both plots are dimensionless time measured in units of $\frac{1}{4\omega_r}$.

ACKNOWLEDGMENTS

The authors thank the Robert A. Welch Foundation (Grant No. F-1051) and the Engineering Research Program of the Office of Basic Energy Sciences at the U.S. Department of Energy (Grant No. DE-FG03-94ER14465) for support of this work. The authors thank the Texas Advanced Computing Center (TACC) for the use of their computing facilities in performing calculations for this paper.

APPENDIX A: EXPERIMENTAL CREATION OF THE EFFECTIVE HAMILTONIAN

In this Appendix, we show how the effective Hamiltonian in Eq. (4) can be used to describe an experimental system of lasers impinging on noninteracting alkali atoms. This analysis involves the consideration of a two-level subsystem of the atom's electronic levels, application of the rotating-wave approximation, and adiabatic elimination of the excited level, to obtain a spatially and temporally periodic potential for atoms in the ground state.

We begin by considering the Hamiltonian of this two-level system, in dipole interaction with a z-polarized classical electric field,

$$H = H_{\rm atom} + H_{\rm int}, \tag{A1}$$

with

$$H_{\rm atom} = \hbar\omega_{at}|e\rangle\langle e| + \frac{p_x^2}{2m}(|e\rangle\langle e| + |g\rangle\langle g|), \tag{A2}$$

and

$$H_{\rm int} = -dE_z(x,t)(|e\rangle\langle g| + |g\rangle\langle e|), \tag{A3}$$

where $\hbar\omega_{at}$ is the energy spacing of the two levels, p_x is the atomic momentum operator in the x direction, and $d \equiv \langle e|\hat{d}_z|g\rangle = \langle g|\hat{d}_z|e\rangle$ is the dipole matrix element coupling the ground state $|g\rangle$ to the excited state $|e\rangle$. The total electric field amplitude $E_z(x,t)$ is assumed to be the superposition of the electric fields due to N lasers, all polarized along the z direction, so that

$$E_z(x,t) = \sum_{j=1}^{N} E^{(j)} \cos\left[\left(k_L + \frac{\delta k_j}{2}\right)x + \sigma_j\left(\omega_L + \frac{\delta\omega_j}{2}\right)t + \phi_j\right], \tag{A4}$$

where $E^{(j)}$ is the amplitude of the jth laser, ω_L is a positive reference frequency, and k_L its corresponding wave number, σ_j can be ± 1, and $\delta k_j = \delta\omega_j/c$ (the usefulness of this form will be evident below). We can then write

$$E_z(x,t) = A(x,t)e^{-i\omega_L t} + A^\star(x,t)e^{i\omega_L t}, \tag{A5}$$

with

$$A(x,t) = \sum_j \frac{E^{(j)}}{2} \exp\left\{-i\sigma_j\left[\left(k_L + \frac{\delta k_j}{2}\right)x + \sigma_j\frac{\delta\omega_j}{2}t + \phi_j\right]\right\}. \tag{A6}$$

Under a time-dependent unitary transformation of the Schrödinger equation, the Hamiltonian transforms like

$$H \to UHU^\dagger + i\hbar\frac{\partial U}{\partial t}U^\dagger. \tag{A7}$$

Using the unitary matrix

$$U = \exp(i\omega_L|e\rangle\langle e|t), \tag{A8}$$

to transform to the rotating frame of the laser leaves the Hamiltonian as

$$H = \hbar\Delta|e\rangle\langle e| + \frac{p_x^2}{2m}(|e\rangle\langle e| + |g\rangle\langle g|) - dE_z(x,t)(|e\rangle\langle g|e^{i\omega_L t} + |g\rangle\langle e|e^{-i\omega_L t}), \quad \text{(A9)}$$

where $\Delta = \omega_{at} - \omega_L$ is the detuning of the reference laser frequency from the atomic transition.

Let us now make the rotating wave approximation by inserting the form of E_z in Eq. (A5) and neglecting terms with high-frequency exponential dependence (i.e., $e^{\pm i2\omega_L t}$). The Hamiltonian then takes the form

$$H = \hbar\Delta|e\rangle\langle e| + \frac{p_x^2}{2m}(|e\rangle\langle e| + |g\rangle\langle g|) - d[A(x,t)|e\rangle\langle g| + A^*(x,t)|g\rangle\langle e|]. \quad \text{(A10)}$$

Writing an arbitrary state $|\psi\rangle = \psi_g(x,t)|g\rangle + \psi_e(x,t)|e\rangle$, the Schrödinger equation can be written

$$i\hbar\frac{\partial\psi_g}{\partial t} = -\frac{\hbar^2}{2m}\frac{\partial^2}{\partial x^2}\psi_g - dA^*(x,t)\psi_e, \quad \text{(A11)}$$

$$i\hbar\frac{\partial\psi_e}{\partial t} = -dA(x,t)\psi_g + \left(\hbar\Delta - \frac{\hbar^2}{2m}\frac{\partial^2}{\partial x^2}\right)\psi_e. \quad \text{(A12)}$$

Adiabatic elimination of the excited state is performed by assuming that the detuning of the laser Δ is large enough to allow us to neglect the time and space derivatives of the excited state. Thus, atoms prepared in the ground state will remain there and we are left with an *effective Hamiltonian* for their evolution,

$$i\hbar\frac{\partial\psi_g}{\partial t} = H_{\text{eff}}\psi_g, \quad H_{\text{eff}} = \frac{p_x^2}{2m} - \frac{d^2|A(x,t)|^2}{\hbar\Delta}. \quad \text{(A13)}$$

The particular form of $A(x,t)$ will depend on the choice of lasers. A pair of counterpropagating lasers with equal carrier frequencies $(E^{(1)} = E^{(2)} \equiv E;\ \delta\omega_1 = \delta\omega_2 = 0;\ \sigma_1 = -\sigma_2;\ \phi_1 = \phi_2 = 0)$ will produce a time-independent, periodic potential, i.e.,

$$A_{\text{stand}}(x,t) = E\cos(k_L x) \rightarrow |A_{\text{stand}}(x,t)|^2 \sim \frac{E^2}{2}\cos(2k_L x), \quad \text{(A14)}$$

where we have neglected constant terms. Similarly, two counterpropagating lasers with slightly offset frequencies $(E^{(1)} = E^{(2)} \equiv E;\ \delta\omega_1 = -\delta\omega_2 \equiv \delta\omega;\ \sigma_1 = -\sigma_2;\ \phi_1 = \phi_2 = 0)$ will produce a traveling periodic potential,

$$A_{\text{trav}}(x,t) = \frac{E}{2}\{e^{i\{[k_L + (\delta k/2)]x - (\delta\omega/2)t\}} + e^{-i\{[k_L - (\delta k/2)]x - (\delta\omega/2)t\}}\} \rightarrow |A_{\text{trav}}(x,t)|^2 \sim \frac{E^2}{2}\cos(2k_L x - \delta\omega t). \quad \text{(A15)}$$

If we combine these two pairs of lasers, we create an effective potential with the desired terms of Eq. (4), namely

$$H = \frac{p_x^2}{2m} - \frac{d^2E^2}{2\hbar\Delta}[\cos(2k_L x) + \cos(2k_L x - \delta\omega t)]. \quad \text{(A16)}$$

It is clear, however, that the $|A(x,t)|^2$ for such a system will also contain unwanted cross terms, which we have neglected in writing Eq. (A16). In order to minimize the effect of these cross terms, we offset the carrier frequency of the second pair by some amount $\Delta\omega$ $(E^{(1)} = E^{(2)} = E^{(3)} = E^{(4)} \equiv E;\ \delta\omega_1 = \delta\omega_2 = 0;\ \delta\omega_3 = \Delta\omega + \delta\omega;\ \delta\omega_4 = \Delta\omega - \delta\omega;\ \sigma_1 = \sigma_3 = -\sigma_2 = -\sigma_4;$ and $\phi_i = 0\ \forall\, i)$, where $\omega_L \gg \Delta\omega \gg \delta\omega$. This yields,

$$|A_{\text{two-res}}(x,t)|^2 \sim \frac{E^2}{2}[\cos(2k_L x) + \cos(2k_L x - \delta\omega t) + \cos(\Delta k x)\cos(\Delta\omega t) + \cos(2k_L x)\cos(\Delta\omega t)], \quad \text{(A17)}$$

where $\Delta k = \Delta\omega/c$ and we have retained only the highest-order terms in the frequencies and wave numbers (e.g., $\delta\omega$ is neglected in the presence of $\Delta\omega$). The last two terms in this equation present high-frequency oscillations, depending on the particular value of $\Delta\omega$. As a concrete example, we can consider a system of cesium atoms. In Refs. [23,24], the laser light was detuned by $\Delta \sim 10^{11}$ Hz from the D_2 line $(\omega_L \sim 10^{15}$ Hz) and a modulation of $\delta\omega \sim 10^5$ Hz was applied to the standing lattice to affect traveling terms in the effective potential. Therefore, an offset of the carrier frequency for the second pair of lasers in the hundreds of MHz will satisfy $\Delta \gg \Delta\omega \gg \delta\omega$, and allow one to safely neglect the last two terms in the square brackets of Eq. (A17) [25].

In order to obtain the Hamiltonian in Eq. (4), we change to dimensionless variables $(p', x', t', \omega'$ and $H')$ as follows. Let $p' = \frac{p_x}{2\hbar k_L}$, $x' = 2k_L x$, $t' = 4\omega_r t$, $\omega' = \frac{1}{4\omega_r}\delta\omega$, and $H' = \frac{1}{4\hbar\omega_r}H$, where the recoil frequency of an atom is $\omega_r = \frac{\hbar k_L^2}{2m}$. The Hamiltonian in Eq. (A16) then takes the form

$$H' = (p')^2 + \kappa[\cos(x') + \cos(x' - \omega' t')], \quad \text{(A18)}$$

where $\kappa \equiv -\frac{d^2E^2}{8\omega_r\hbar^2\Delta}$ Removing the primes, we obtain the desired Hamiltonian. Dimensionless energies and Floquet eigenvalues will be measured in units of $4\hbar\omega_r$. In these units, the effective Planck's constant is unity. It is important to note that with this choice of dimensionless units, changes in momentum due to the interaction of an atom with the lasers are integer valued. Moreover, experimental techniques allow for the preparation of atoms in a very narrow range of momentum values about zero [23,24,26]. Therefore, the eigenvalues of the momentum operator will take only integer values, i.e., $\hat{p}|n\rangle = n|n\rangle$ with $n \in \mathbb{Z}$.

APPENDIX B: "EVOLUTION" OF A FLOQUET HAMILTONIAN

In this Appendix, the (t,t') formalism due to Peskin and Moiseyev [27,28] is used to justify the time parametrization of κ_1 and κ_2 in the model Hamiltonians in Eqs. (24) and (51). These models are each subsystems of a *Floquet* Hamiltonian which was constructed under the assumptions that κ_1 and κ_2 were constant and the Schrödinger equation was time peri-

odic. The subsequent parametrization of such a system by nonperiodic functions of time therefore requires a more rigorous explanation. Here, we show that a physical system represented by a Hamiltonian with both periodic and arbitrary dependence on time, can be associated to Floquet-like Hamiltonian in an extended Hilbert space where the periodic time dependence has been reduced to dependence on a coordinate. This Hamiltonian is termed "Floquet-like" because its dependence on the *coordinate* time is identical to a Floquet Hamiltonian's dependence on time. The remaining arbitrary time dependence of the Floquet-like Hamiltonian determines, via the Schrödinger equation, a dynamics in the extended space from which the dynamics of the original system can be recovered.

Consider the Schrödinger equation for a time-dependent Hamiltonian

$$i\frac{\partial}{\partial t}\psi(x;t) = H(x;t)\psi(x;t), \tag{B1}$$

where x can be considered a single spatial coordinate or a set of coordinates and $\hbar$ has been set to unity by nondimensionalization of the variables. We will associate to $H(x;t)$ a Hamiltonian of one more coordinate $H_F(x,t';t)$ which is a Hermitian operator in a larger Hilbert space, extended to include this new coordinate t'. The relationship between the two Hamiltonians is defined by

$$H_F(x,t';t) = \bar{H}(x,t';t) - i\frac{\partial}{\partial t'}, \tag{B2}$$

with

$$\bar{H}(x,t';t)|_{t'=t} = H(x;t). \tag{B3}$$

Clearly, $H(x;t)$ does not uniquely determine $H_F(x,t';t)$. The time evolution of a state $\bar{\psi}(x,t';t)$ in the extended space is governed by the Schrödinger equation

$$i\frac{\partial}{\partial t}\bar{\psi}(x,t';t) = H_F(x,t';t)\bar{\psi}(x,t';t), \tag{B4}$$

which can also be written

$$i\left[\left(\frac{\partial}{\partial t} + \frac{\partial}{\partial t'}\right)\bar{\psi}(x,t';t)\right] = \bar{H}(x,t';t)\bar{\psi}(x,t';t). \tag{B5}$$

If we take this equation at the cut $t'=t$, it becomes

$$i\frac{\partial}{\partial t}[\bar{\psi}(x,t';t)|_{t'=t}] = H(x;t)[\bar{\psi}(x,t';t)|_{t'=t}], \tag{B6}$$

where we have used the identity

$$\frac{\partial}{\partial t}[\bar{\psi}(x,t';t)|_{t'=t}] = \left[\left(\frac{\partial}{\partial t} + \frac{\partial}{\partial t'}\right)\bar{\psi}(x,t';t)\right]_{t'=t}. \tag{B7}$$

Comparing Eqs. (B6) and (B1), we see that the evolution of a state in the original system can be determined by evolution in the extended system using

$$\psi(x;t) = \bar{\psi}(x,t';t)|_{t'=t}, \tag{B8}$$

and provided the same initial condition

$$\bar{\psi}(x,t';t)|_{t'=t=0} = \psi(x,0) \tag{B9}$$

is used in each space.

We now apply this formalism to STIRAP transitions in the two-resonance Hamiltonian. The evolution plotted in Fig. 9(b) was performed by numerical integration of the Schrödinger equation, using the Hamiltonian

$$H(x;t) = -\frac{\partial^2}{\partial x^2} + \kappa_0[\cos x + \cos(x-\omega_0 t)] + \lambda\cos x[\kappa_1(t)\cos(\Omega_1 t) + \kappa_2(t)\cos(\Omega_2 t)], \tag{B10}$$

where κ_1 and κ_2 were given Gaussian time dependence in order to affect the STIRAP-like transition. The solid lines plotted in Fig. 9(a), were determined by evolution of a Schrödinger equation using the time-parametrized three-level model in Eq. (51). Using the above analysis we can show that, modulo the perturbation theory approximations, these two methods of time-evolution are equivalent. We define a Hamiltonian in the extended space

$$\bar{H}(x,t';t) = -\frac{\partial^2}{\partial x^2} + \kappa_0[\cos x + \cos(x-\omega_0 t')] + \lambda\cos x[\kappa_1(t)\cos(\Omega_1 t') + \kappa_2(t)\cos(\Omega_2 t')], \tag{B11}$$

which satisfies Eq. (B3) for the two-resonance Hamiltonian and has the property that functions periodic in time are now functions of the extra coordinate, while the amplitudes of the modulations are functions of the usual time parameter. The full Hamiltonian in the extended space $H_F(x,t';t)$, defined by Eq. (B2), has the same dependence on t' that the Floquet Hamiltonian in Eq. (29) has on time t. Therefore, the entire perturbation analysis performed on the Floquet Hamiltonian in Sec. III would proceed in identical fashion on $H_F(x,t';t)$, yielding a time-parametrized three-level model. If Eqs. (B8) and (B9) are satisfied, the "time-parametrized" Floquet Hamiltonian can be used to determine the physical evolution.

[1] U. Gaubatz, P. Rudecki, M. Becker, S. Schiemann, M. Külz, and K. Bergmann, Chem. Phys. Lett. **149**, 463 (1988).
[2] U. Gaubatz, P. Rudecki, M. Becker, S. Schiemann, and K. Bergmann, J. Chem. Phys. **92**, 5363 (1990).
[3] N. V. Vitanov, T. Halfmann, B. W. Shore, and K. Bergmann, Annu. Rev. Phys. Chem. **52**, 763 (2001).
[4] P. Marte, P. Zoller, and J. L. Hall, Phys. Rev. A **44**, R4118 (1991).
[5] L. S. Goldner, C. Gerz, R. J. C. Spreeuw, S. L. Rolston, C. I. Westbrook, W. D. Phillips, P. Marte, and P. Zoller, Phys. Rev.

Lett. **72**, 997 (1994).
[6] M. Weitz, B. C. Young, and S. Chu, Phys. Rev. Lett. **73**, 2563 (1994).
[7] T. Esslinger, F. Sander, M. Weidemüller, A. Hemmerich, and T. W. Hänsch, Phys. Rev. Lett. **76**, 2432 (1996).
[8] S. Kulin, B. Saubamea, E. Peik, J. Lawall, T. W. Hijmans, M. Leduc, and C. Cohen-Tannoudji, Phys. Rev. Lett. **78**, 4185 (1997).
[9] K. Na and L. E. Reichl, Phys. Rev. A **70**, 063405 (2004).
[10] K. Na and L. E. Reichl, Phys. Rev. A **72**, 013402 (2005).
[11] K. Na, C. Jung, and L. E. Reichl, J. Chem. Phys. **125**, 034301 (2006).
[12] J. R. Kuklinski, U. Gaubatz, F. T. Hioe, and K. Bergmann, Phys. Rev. A **40**, R6741 (1989).
[13] F. T. Hioe, Phys. Lett. **99A**, 150 (1983).
[14] J. Oreg, F. T. Hioe, and J. H. Eberly, Phys. Rev. A **29**, 690 (1984).
[15] C. E. Carroll and F. T. Hioe, J. Math. Phys. **29**, 487 (1988).
[16] K. Eckert, M. Lewenstein, R. Corbalán, G. Birkl, W. Ertmer, and J. Mompart, Phys. Rev. A **70**, 023606 (2004).
[17] R. Graham, M. Schlautmann, and P. Zoller, Phys. Rev. A **45**, R19 (1992).
[18] M. Abramowitz and I. A. Stegun, *Handbook of Mathematical Functions*, Applied Mathematics Series No. 55 (U.S. Department of Commerce, Washington, DC, 1972).
[19] H. Sambe, Phys. Rev. A **7**, 2203 (1973).
[20] A. Ya. Dzyublik, Theor. Math. Phys. **87**, 393 (1991).
[21] B. P. Holder and L. E. Reichl, Phys. Rev. A **72**, 043408 (2005).
[22] K. Husimi, Proc. Phys. Math. Soc. Jpn. **22**, 264 (1940).
[23] D. A. Steck, W. H. Oskay, and M. G. Raizen, Science **293**, 274 (2001).
[24] D. A. Steck, W. H. Oskay, and M. G. Raizen, Phys. Rev. Lett. **88**, 120406 (2002).
[25] M. G. Raizen (private communication).
[26] M. Kasevich and S. Chu, Phys. Rev. Lett. **69**, 1741 (1992).
[27] U. Peskin and N. Moiseyev, J. Chem. Phys. **99**, 4590 (1993).
[28] A. Fleischer and N. Moiseyev, Phys. Rev. A **72**, 032103 (2005).